

Tien, C., C.-S. Wang and D. T. Barot, "Chainlike Formation of Particle Deposits in Fluid-Particle Separation," *Science*, **196**, 983 (1977).
 Wang, C.-S., M. Beizaie and C. Tien, "Deposition of Solid Particles on a Collector: Formulation of a New Theory," *AIChE J.*, **23**, 879 (1977).
 Watson, J. H. L., "Filmless Sample Mounting for the Electron Microscope," *J. Appl. Phys.*, **17**, 121 (1946).

Yoshioka, N., H. Emi and M. Yasunami, "Filtration of Aerosols through Fibrous Packed Bed with Dust Loading," *Kagaku Kōgaku*, **33**, 1013 (1969).

Manuscript received August 3, 1979; revision received February 1, and accepted February 29, 1980.

Effect of Electrostatic Fields on Accumulation of Solid Particles on Single Cylinders

C. S. WANG

and

C. P. HO

Department of Chemical Engineering
 and Materials Science
 Syracuse University
 Syracuse, New York 13210

and

H. MAKINO

and

K. IINOYA

Department of Chemical Engineering
 Kyoto University, Kyoto 606 Japan

When a particle laden gas flows past a transverse fiber, such as in a fibrous filter, particles are captured first on the surface of the fiber and later on the deposited particles as well. Watson (1946) observed that solid particles tend to build up on the surface of a collector in dendritic form. The rates at which solid spheres accumulate on single fibers and the morphology of particle deposits, in the absence of electrostatic fields, were studied by Billings (1966) and Barot et al. (1980).

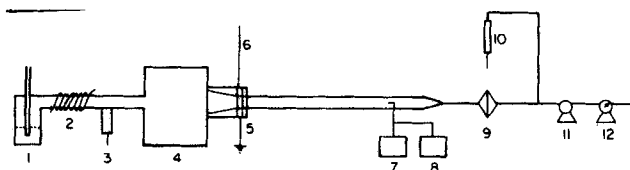
The tendency for deposits to grow in dendritic form is a consequence of two intrinsic properties of aerosols: the particles have finite sizes and the particles are randomly distributed in the aerosol stream. When the trajectory of a particle approaching a transverse fiber is intercepted by a particle already deposited on the fiber, the oncoming particle is captured by the deposited particle, and a two-particle chain is formed. Based on these concepts, Tien et al. (1977) developed a general theory for the accumulation of solid particles on an obstacle in a stream of fluid-solid suspension.

In the presence of electrostatic forces, the rate at which particles accumulate on a fiber is markedly increased, but the tendency for deposits to grow in dendritic form remains unchanged. This note presents the results of an experimental study of the accumulation of particles on single fibers and the

morphology of particle deposits, in the presence of electrostatic fields.

EQUIPMENT AND METHODS

Figure 1 shows the general arrangement of the experimental setup used in this study. Monodisperse aerosols of polyvinyl



- | | |
|------------------------------------|--------------------------------|
| 1 COLLISION-TYPE AEROSOL GENERATOR | 7 BAUSCH-LOMB PARTICLE COUNTER |
| 2 HEATING SECTION | 8 PARTICLE MASS MONITOR |
| 3 SONIC JET IONIZER | 9 FILTER |
| 4 MIXING CHAMBER | 10 ROTAMETER |
| 5 TEST SECTION | 11 VACUUM PUMP |
| 6 H.V. SUPPLY | 12 WET TEST METER |

Figure 1. Experimental apparatus.

Correspondence concerning this note should be addressed to C. S. Wang.

0001-1541-80-3915-0680-\$00.75. © The American Institute of Chemical Engineers, 1980.

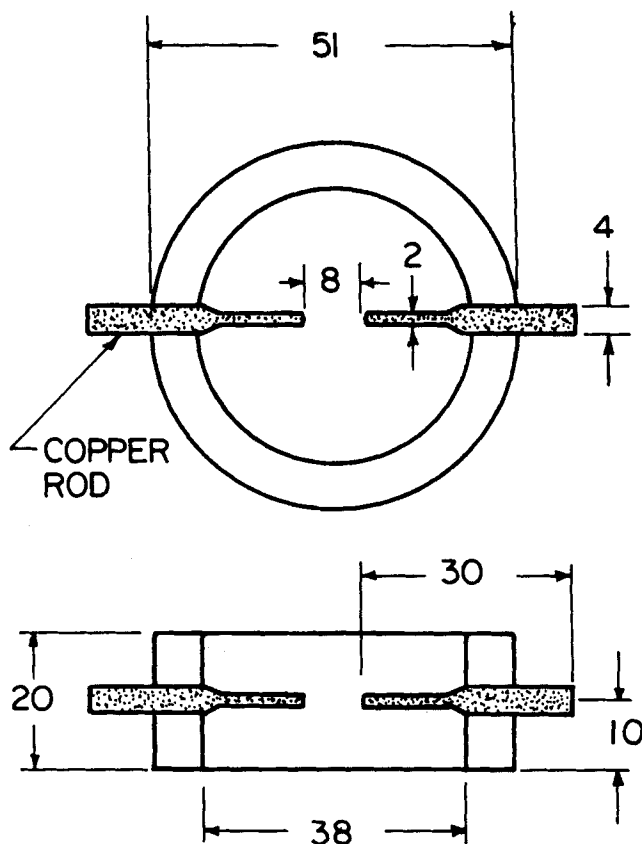


Figure 2. Fiber holder. Dimension in mm.

toluene spheres, $2.02\ \mu\text{m}$ in diameter, were produced from liquid suspensions by means of a Collison nebulizer. The droplet laden gas stream, $7.2\ \text{l/min}$, from the nebulizer was passed through a heating section and then mixed with a dry air stream, $44.4\ \text{l/min}$, from a sonic jet ionizer. The resulting aerosols, which contained particles with electric charges at the Boltzmann distribution, were then led into a mixing chamber. Excess aerosols were exhausted from the chamber through cloth filters.

The test section was connected to the mixing chamber by a convergent coneshaped duct to give a uniform flow. Shown in Figure 2 is a fiber holder which constituted the main part of the test section. The glass fiber, $8.5\ \mu\text{m}$ in diameter, was mounted on the holder by glueing the two ends of the fiber to the bars which protruded inward from the ring.

Parallel electrostatic fields were provided by placing two 12 mesh copper screens at right angles to the flow, with the upstream screen connected to a high voltage supply and the downstream screen grounded. The glass fiber was mounted at a point $0.42\ \text{cm}$ downstream of the first screen and $0.54\ \text{cm}$ upstream of the second. The screens were made of copper wires, $0.4\ \text{mm}$ in diameter.

Cross-flow electrostatic fields were applied through two $0.8\ \text{mm}$ thick copper plates, $0.99\ \text{cm}$ apart.

The particle concentration of test aerosols was determined by an aerosol mass monitor. The readings, in milligrams per cubic meters, were converted to number concentrations for spheres, $2.02\ \mu\text{m}$ in diameter and $1.027\ \text{g/cm}^3$ in density. A Bausch and Lomb optical counter was also used. Under the experimental conditions, the particle concentrations were too high for the optical counter, and therefore a correlation chart between the counter readings and the mass concentrations was used to determine the actual number concentrations.

In each run, the fiber was removed with the holder from the test section at intervals of 2 to 4 min for observation and photo-

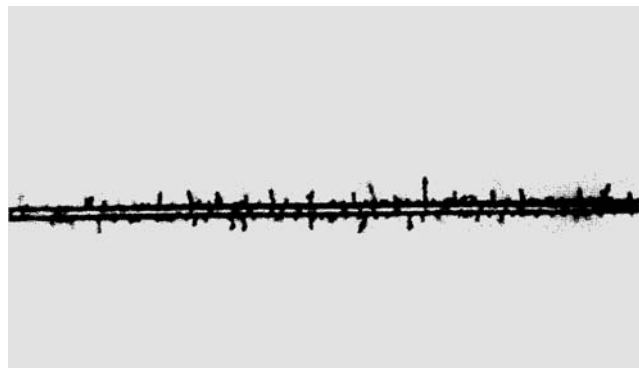


Figure 3. Deposits on a section of fiber No. 4 at $t = 6\ \text{min}$. graphing under an optical microscope (with a $10\times$ objective and $20\times$ eyepieces).

RESULTS

Figure 3 is a photograph taken of fiber No. 4 after it had been exposed to an aerosol flow for 6 min. The picture was taken from the upstream side. The electrostatic field, $5\ \text{kV/cm}$, was normal to the flow and the fiber, with the high voltage on the top side of the photograph.

The number of dendrites formed over $355\ \mu\text{m}$ of a fiber (the length shown in each picture) and the number of particles in each dendrite were counted from each photograph. At the end of each time interval in a run, three sections of the fiber were photographed from four different angles: 0° , 45° , 90° and 135° from the forward stagnation point. The counts from the photograph of 0° were added to the counts from those of 90° , and the counts from the photograph of 45° were added to those of 135° . The results are shown in Figures 4 and 5. The number of particles crossing the projected area of a fiber section of $355\ \mu\text{m}$, instead of time, is used as the abscissa. The results

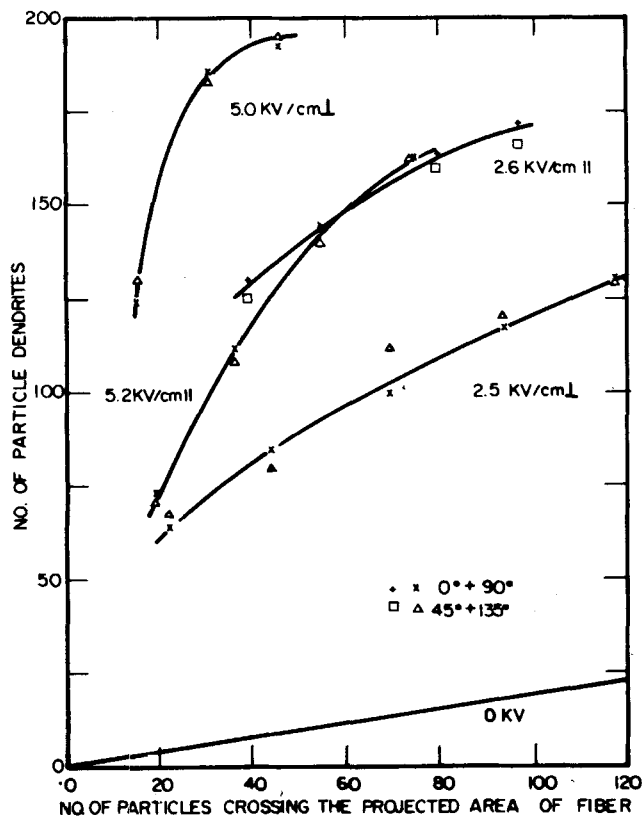


Figure 4. Number of dendrites over $355\ \mu\text{m}$ of a fiber as a function of number of particles crossing the projected area of fiber. The curve for $0\ \text{kv}$ is based on data of Barot et al. (1980), obtained under the same conditions as this study, except that the air velocity was $23.4\ \text{cm/s}$.

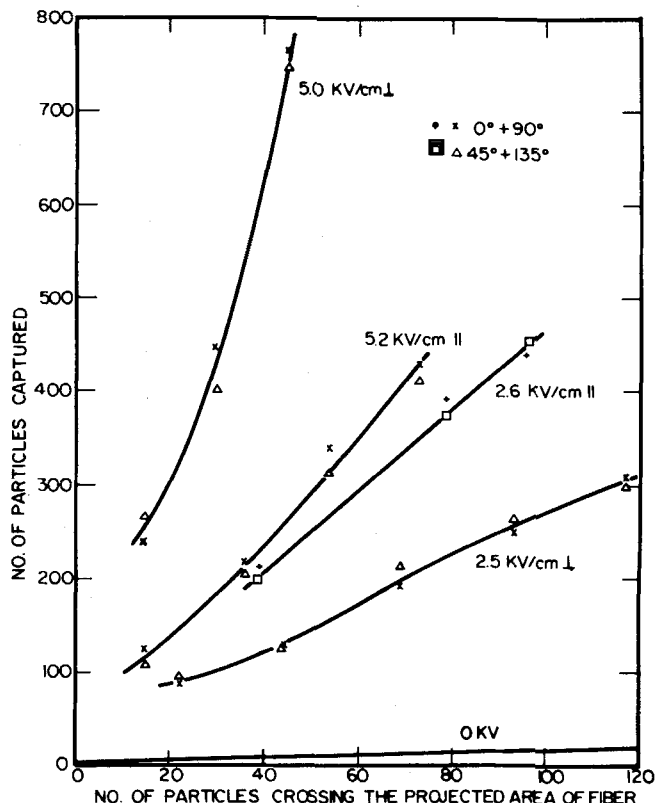


Figure 5. Number of particles captured over $355\ \mu\text{m}$ of a fiber as a function of particles crossing the projected area of fiber. The curve for $0\ \text{kv}$ is based on data of Barot et al. (1980).

TABLE 1. EXPERIMENTAL CONDITIONS

Fiber No.	Electrostatic field,* kv/cm	Aerosol Concentration particles/cm ³
1	2.6	191
2	5.2	186
3	2.5 ⊥	160
4	5.0 ⊥	153

* An electrostatic field parallel to the flow is indicated by ||, while a field normal to the flow and the fiber is indicated by ⊥.

All four fibers were 8.5 μm in diameter (d_f). The particles were 2.02 μm in diameter (d_p) and the air velocity (v) 27 cm/s. The corresponding values of the flow Reynolds number, the Stokes number and the relative size were:

$$Re = \frac{dv}{\nu} = 0.15$$

$$St = \frac{C\rho_p v d_p^2}{9\mu d_f} = 0.81$$

$$R = \frac{d_p}{d_f} = 0.237$$

where ν is the kinematic viscosity of air, ρ_p the particle density, C the Cunningham correction factor and μ the viscosity of air.

indicate that the counts from pictures of 0 and 90 deg are in good agreement with those of 45 and 135 deg. It is therefore assumed that these counts can represent the numbers of dendrites and particles over a fiber section of 355 μm. The validity of this assumption has not been tested. It is likely that a short dendrite can be formed on such a location that it would not appear in either of the two pictures taken from 0 and 90 deg (or 45 and 135 deg). But it is also likely that a long dendrite can be formed on such a location that it would appear in both pictures. The first situation leads to an underestimate, while the second leads to an overestimate of the number of dendrites.

DISCUSSIONS

The dendrites formed in the presence of electrostatic fields are generally in the form of straight chains. This is in contrast to the irregularly shaped dendrites formed in the absence of electrostatic fields. The difference in the manner in which the dendrites grow is clearly a result of the difference in force fields.

Figures 4 and 5 show that curves for the number of dendrites are concave downwards, while curves for the total number of particles captured generally concave upwards. This implies that the number of dendrites reached a plateau after a rapid buildup at the beginning, whereas the collection efficiency continued to increase within the time periods studied.

The collection efficiency of a fiber is defined as the thickness of the layer in the undisturbed flow far upstream of the fiber, from which all aerosol particles are deposited, divided by the fiber diameter. This definition has been used for both clean and loaded fibers. If N represents the number of particles captured by a section of fiber in a given time period and N_0 the number of particles crossing the projected area of that section of fiber during the same time period, the collection efficiency of the fiber is simply the slope of the curve of N against N_0 :

$$\eta = \frac{dN}{dN_0}$$

Because of uncertainties in extrapolation of data back to time $t = 0$, the collection efficiency of a clean fiber cannot be accurately determined from Figure 5. The efficiency of a loaded fiber, with the number of particles captured falling in the range covered in experiments, can be easily estimated. For instance, the slopes at $N = 250$ for the four curves in Figure 5 were found to be

1. $\eta = 4.3$ for $E = 2.6$ kv/cm ||
2. $\eta = 5.7$ for $E = 5.2$ kv/cm ||
3. $\eta = 2.3$ for $E = 2.5$ kv/cm ⊥
4. $\eta = 10.2$ for $E = 5.0$ kv/cm ⊥

The collection efficiency exceeds one for all cases, indicating

that the thickness of the layer from which all the aerosol particles were captured was greater than the diameter of the fiber.

The collection efficiency of a fiber placed in an electrostatic field is higher than in the absence of electric fields. According to the data of Barot et al. (1980), the collection efficiency of an 8.5 μm glass fiber for 2.02 μm polyvinyl toluene spheres in the absence of electrostatic fields was 0.24 at $N = 200$ and an air velocity of 23.4 cm/s. It is seen that an electrostatic field of 2.6 kv/cm parallel to air flow increases the collection efficiency by a factor of about 20.

If a uniform electric field is applied across an isolated, uncharged cylinder, the latter is polarized and the field becomes nonuniform. The resulting field has influences on both charged and uncharged particles. A theory for deposition of point particles on such a cylinder has been worked out by Zebel (1965), using both potential flow and the Lamb solution for viscous flow transverse to a circular cylinder.

Zebel's theory is valid only when the Stokes number, which indicates the importance of particle inertia, and the relative size, an index of interception effect, both vanish. In the present study, the values of St and R were 0.81 and 0.237, respectively (Table 1), too large to be neglected.

In an attempt to predict the efficiency of a fiber placed in an electric field, the equation of motion was solved numerically for uncharged particles of finite size, taking into account the particle inertia. The electric force on the particle due to polarization was approximated by the expression derived for particles much smaller than the radius of the cylinder. Davies' solution (1950) for viscous flow transverse to a cylinder was used and the initial position of a particle was placed at 200 radii upstream of the fiber, where the flow was nearly uniform. At a flow Reynolds number of 0.15 (Table 1), there is reverse flow downstream of the cylinder. The calculated efficiencies of clean fibers for the conditions listed in Table 1 are as follows:

1. $\eta_0 = 0.076$ for $E = 2.6$ kv/cm ||
2. $\eta_0 = 0.091$ for $E = 5.2$ kv/cm ||
3. $\eta_0 = 0.074$ for $E = 2.5$ kv/cm ⊥
4. $\eta_0 = 0.088$ for $E = 5.0$ kv/cm ⊥

These values are, on average, about 1/50 of the experimentally determined efficiencies for loaded fibers at $N = 250$. To examine the interception effect of particle dendrites on collection efficiency, calculations were made for a fiber with two ten-particle dendrites, one at 90 deg and the other at -90 deg from the forward stagnation point. The particles were assumed to move along the same trajectories as they would in the absence of dendrites. The effects of dendrites on the flow field and the electrical field were not considered. The calculated efficiencies for the conditions in Table 1 are

1. $\eta = 2.195$ for $E = 2.6$ kv/cm ||
2. $\eta = 2.195$ for $E = 5.2$ kv/cm ||
3. $\eta = 2.190$ for $E = 2.5$ kv/cm ⊥
4. $\eta = 2.205$ for $E = 5.0$ kv/cm ⊥

which are about one half of the experimental values for loaded fibers at $N = 250$. It is seen that the calculated efficiencies increase by a factor of about 25, although the two ten-particle dendrites extend the diameter of the fiber only by a factor of 5.74. The marked effect of interception by dendrites is a result of the fact that particles moving far off center have nearly rectilinear trajectories. However, the interception effect alone cannot explain the significant difference in experimental efficiencies between normal and parallel electric fields.

ACKNOWLEDGMENT

The work was partly supported by NSF Award Number INT77-14422 from the National Science Foundation. The experiments were carried out in Professor K. Iinoya's Laboratory, Department of Chemical Engineering, Kyoto University, Kyoto, Japan, where C. S. Wang spent his sabbatical leave from January 5 to June 30, 1978. C. S. Wang is grateful to Dr. K. Makino, Dr. H. Yoshida and Dr. K. Ushiki for providing assistance in the experiments.

LITERATURE CITED

- Barot, D. T., C. Tien and C. S. Wang, "Accumulation of Solid Particles on Single Fibers Exposed to Aerosol Flows," *AIChE J.*, **26**, 289 (1980).
- Billings, C. E., "Effects of Particle Accumulation in Aerosol Filtration," Ph.D. dissertation, Calif. Inst. Technol., Pasadena (1966).
- Davies, C. N., "Viscous Flow Transverse to a Circular Cylinder," *Proc. Phys. Soc. (London)*, **B63**, 288 (1950).
- Tien, C., C. S. Wang and D. T. Barot, "Chain-like Formation of Particle Deposits in Fluid-Particle Separation," *Science*, **196**, 983 (1977).
- Watson, J. H. L., "Filmless Sample Mounting for the Electron Microscope," *J. Appl. Phys.*, **17**, 121 (1946).
- Zebel, G., "Deposition of Aerosol Flowing past a Cylindrical Fiber in a Uniform Electric Field," *J. Colloid. Sci.*, **20**, 522 (1965).

Manuscript received October 1, 1979; revision received February 12, and accepted February 29, 1980.

Combined Laminar Forced and Free Convection Heat Transfer to Viscoelastic Fluids

A. V. SHENOY

CEPD Division
National Chemical Laboratory
Pune 411 008, India

$$\theta = \frac{T - T_\infty}{T_w - T_\infty}$$

and

$$Wi = \frac{2m}{\rho} \frac{U_\infty^{s-2}}{l_c^2} \quad (4)$$

$$Pr = \frac{\rho C_p}{k} \left(\frac{K}{\rho} \right)^{\frac{1}{n}} U_\infty^{\frac{2(n-1)}{n}} \quad (5)$$

The choice of the constitutive equation is the same as that of Shenoy and Mashelkar (1978) in their analysis of laminar natural convection heat transfer to a viscoelastic fluid and the above Equations (1) and (2) are generated by similar arguments. The boundary conditions on the velocity and temperature profiles are

$$\begin{aligned} u_1(x_1, 0) &= 0 & u_1(x_1, \delta_1) &= 0 \\ \theta(x_1, 0) &= 0 & \theta(x_1, \delta_{T_1}) &= 0 \end{aligned} \quad (6)$$

In line with the general tradition of an integral solution, the

A correlating equation for combined laminar forced and free convection heat transfer to Newtonian fluids was proposed by Churchill (1977) and supported by Ruckenstein (1978). It was further shown by Shenoy (1980) that the same equation could be used for non-Newtonian power-law fluids except for the new definitions of Nusselt numbers for pure forced and free convection respectively. There exists no theoretical analysis of combined laminar forced and free convection heat transfer to viscoelastic fluids and hence the purpose of this communication is to study this problem, providing a sequel to the above efforts. Essentially, the idea is to use the same correlating equation as Churchill (1977), with renewed definitions of Nusselt numbers pertinent to viscoelastic fluids for pure forced and pure free convection respectively.

A theoretical analysis of laminar forced convection heat transfer to viscoelastic fluids is done by the approximate integral method. A similarity solution is obtained and is seen to exist only for the case of a second order fluid in the stagnation region of a constant temperature heated horizontal cylinder. Under exactly the same conditions, Shenoy and Mashelkar (1978) analyzed the laminar natural convection heat transfer to viscoelastic fluids. Using the two informations, an idea of the combined laminar forced and free convection heat transfer to viscoelastic fluids is obtained.

THEORETICAL ANALYSIS

For two-dimensional steady laminar forced convection flow of a viscoelastic fluid over an object indicated in Figure 1, the simplified non-dimensionalised boundary equations of momentum and energy in their integral forms can be written as

$$\begin{aligned} \frac{\partial}{\partial x_1} \int_0^{\delta_1} (u_1^2 - U_1^2) dy_1 &= - \left(\frac{\partial u_1}{\partial y_1} \right)_{y_1=0}^n \\ &+ Wi \frac{\partial}{\partial x_1} \int_0^{\delta_1} \left(\frac{\partial u_1}{\partial y_1} \right)^s dy_1 \end{aligned} \quad (1)$$

$$\frac{\partial}{\partial x_1} \int_0^{\delta_{T_1}} u_1 \theta dy_1 = - \frac{1}{Pr} \left(\frac{\partial \theta}{\partial y_1} \right)_{y_1=0} \quad (2)$$

where

$$\begin{aligned} x_1 &= \frac{x}{l_c}; & y_1 &= \frac{y}{l_c}; & u_1 &= \frac{u}{U_\infty} \\ U_1 &= \frac{U}{U_\infty}; & \delta_1 &= \frac{\delta}{l_c}; & \delta_{T_1} &= \frac{\delta_T}{l_c} \end{aligned} \quad (3)$$

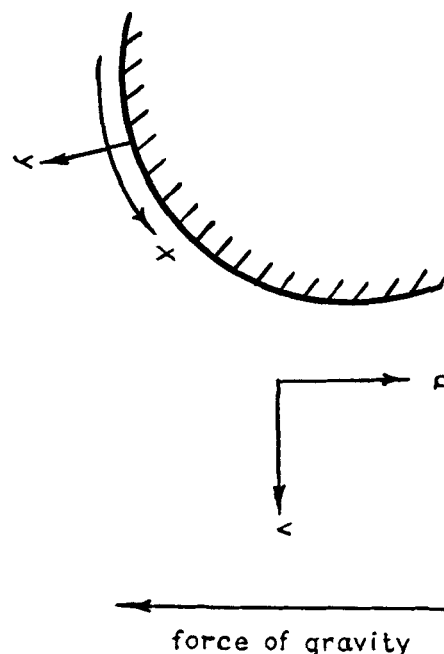


Figure 1. Schematic diagram of flow past a curved surface.